



OPEN

Predictors of residual tricuspid regurgitation after interventional therapy: an automated deep-learning CT analysis

Isabel Mattig^{1,2,3,4}, Elena Romero Dorta^{1,2}, Katherine Fitch⁵, Alexander Lembcke⁶, Marc Dewey^{1,3,4,6,7}, Karl Stangl^{1,2,3} & Henryk Dreger^{2,3,8,9}✉

Computed tomography (CT) is used as a valuable tool for device selection for interventional therapy in tricuspid regurgitation (TR). We aimed to evaluate predictors of TR reduction using CT and automated deep learning algorithms. Patients with severe to torrential TR and CTs prior to either percutaneous annuloplasty (PA) or tricuspid transcatheter edge-to-edge repair (T-TEER) were enrolled. CTs were analyzed using automated deep learning algorithms to assess tricuspid valve anatomy, right heart morphology, and function. Outcome parameters comprised post-interventional TR ≤ 1 and all-cause mortality. 84 patients with T-TEER ($n = 32$) or PA treatment ($n = 52$) were enrolled. Patients with a post-interventional TR ≤ 1 presented lower tenting heights and smaller tenting angles compared to patients with a TR > 1 . Tenting height showed the best accuracy for post-interventional TR > 1 with an AUC of 0.756 (95% CI 0.560–0.951) in the T-TEER and 0.658 (95% CI 0.501–0.815) in the PA group, consistent with a suggested threshold of 6.8 mm and 9.2 mm, respectively. Patients with a post-interventional TR ≤ 1 exhibited a mortality of 4% and those with a TR > 1 of 12% during a follow-up of 331 ± 300 and 370 ± 265 days, respectively ($p = 0.124$). To conclude, tenting is associated with procedural outcomes and should be considered during screening for interventional TR therapy.

Abbreviations

ASE	American Society of Echocardiography
CIED	Cardiac implantable electronic device
CT	Computed tomography
EACVI	European Association of Cardiovascular Imaging
ESC	European Society of Cardiology
PA	Percutaneous annuloplasty
RCA	Right coronary artery
ROC	Receiver operating characteristic
TR	Tricuspid regurgitation
T-TEER	Tricuspid transcatheter edge-to-edge repair

Tricuspid regurgitation (TR) has a significant impact on survival leading to a relevant increase in mortality¹. Particularly in the elderly, the prevalence of TR increases and results in a substantial disease burden². Surgical repair or replacement is effective in TR reduction but also associated with a high intra-hospital mortality rate

¹Department of Cardiology, Angiology and Intensive Care Medicine, Deutsches Herzzentrum der Charité, Campus Charité Mitte, Berlin, Germany. ²Charité – Universitätsmedizin Berlin, Corporate Member of Freie Universität Berlin and Humboldt-Universität zu Berlin, Charitéplatz 1, 10117 Berlin, Germany. ³DZHK (German Centre for Cardiovascular Research), Partner Site, Berlin, Germany. ⁴Berlin Institute of Health at Charité – Universitätsmedizin Berlin, BIH Biomedical Innovation Academy, Berlin, Germany. ⁵Laralab GmbH, Munich, Germany. ⁶Department of Radiology, Charité – Universitätsmedizin Berlin, Corporate Member of Freie Universität Berlin and Humboldt-Universität zu Berlin, Charitéplatz 1, 10117 Berlin, Germany. ⁷Berlin University Alliance, BAU, Berlin, Germany. ⁸Department of Cardiology, Angiology and Intensive Care Medicine, Deutsches Herzzentrum der Charité, Campus Virchow Klinikum, Augustenburger Platz 1, 13353 Berlin, Germany. ⁹Structural Heart Intervention Program (SHIP), Deutsches Herzzentrum der Charité, Berlin, Germany. ✉email: henryk.dreger@dhzc-charite.de

up to 10%³. Consequently, there is a need for new treatment options besides surgical and symptomatic medical therapy. In recent years, new interventional therapies were developed for patients with a high operative risk and demonstrated a significant impact on TR reduction and improvement of functional capacity^{4–9}. Percutaneous annuloplasty (PA) and tricuspid transcatheter edge-to-edge repair (T-TEER) are the most used approaches and several algorithms for device selection have been proposed^{4,8,9}. However, predictors of post-interventional TR reduction remain limited.

Procedural planning is essential for successful interventional therapy. While echocardiography is the primary modality for TR assessment, computed tomography (CT) serves as an alternative method to measure tricuspid valve anatomy, right heart morphology, and function¹⁰. CT assessment is used to evaluate tricuspid annular dimensions, location of leads from cardiac implantable electronic devices (CIEDs) and the proximity of the tricuspid annulus to the right coronary artery (RCA)⁸. Moreover, cardiac CT is necessary to guide the optimal placement of anchor points in patients undergoing PA⁸. In addition to procedural planning, parameters assessed by cardiac CT can predict post-interventional outcome¹¹. Tanaka et al. observed an association between a reduced right ventricular ejection fraction (RVEF) measured by CT and an increase in all-cause mortality and hospitalization due to heart failure 1 year after interventional therapy¹¹.

Since CT is typically performed during TR evaluation and procedural planning of both PA and occasionally T-TEER, integrating its information into treatment algorithms is essential for optimizing patients' therapy and device selection. Therefore, the focus of our current study was to assess tricuspid valve anatomy, right heart morphology, and function by CT using automated deep learning algorithms in patients who underwent PA or T-TEER. Furthermore, we aimed to evaluate parameters associated with residual TR after interventional therapy.

Methods

Study design

We enrolled patients who underwent PA (Cardioband[®], Edwards Lifesciences, Irvine, CA, USA) or T-TEER (TriClip[®], Abbott, Chicago, Illinois, USA, or PASCAL[®], Edwards Lifesciences, Irvine, California, USA) from 2019 to 2023 due to symptomatic severe to torrential TR despite optimal medical therapy. Due to availability of automated CT analysis since 2022, we performed a retrospective analysis of previous cases and a prospective analysis of new patients (2019–2023). Additional inclusion criteria comprised a cardiac full cycle CT during the screening process prior to interventional therapy. Patients with combined procedures of the tricuspid and mitral valve and patients with a second TR procedure (e.g. PA following T-TEER) were excluded from the analysis.

All patients underwent TR evaluation prior to interventional therapy which includes echocardiographic examination, cardiac CT and right and left heart catheterization. The device selection and recommendation of our local heart team was based on the individual tricuspid anatomy and function^{8,9,12}. In detail, PA was mainly chosen in patients with atrial TR, a central jet, and a sufficient distance from the hinge point to the right coronary artery¹². In contrast, patients with ventricular TR, a more commissural jet, and a coaptation gap of less than 8 mm were treated with T-TEER¹². The decision tree is published elsewhere¹². If PA appeared more feasible or T-TEER was challenging or not feasible, patients underwent a complete work-up including a cardiac CT. Moreover, while some of the TR patients seemed to be good candidates for PA based on echocardiography, the CT scan revealed anatomical characteristics such as prohibitive RCA proximity. Accordingly, these patients were treated with T-TEER and CT scans were available for the present analysis. Since establishing a prospective registry, all patients were invited to receive follow-up examinations. Written informed consent was provided by patients with follow-up examinations; the need for written informed consent of patients with retrospective CT analysis was negated by our institutional review board and data protection service. The study was authorized by the institutional review board of the Charité – Universitätsmedizin Berlin, Germany (EA4/218/21 and EA1/043/20) and conducted in accordance with relevant guidelines and regulations, including the Declaration of Helsinki.

Echocardiography was performed in line with the standards of the American Society of Echocardiography (ASE) and the European Association of Cardiovascular Imaging (EACVI)^{13,14}. The assessment comprised right ventricular morphology and function as well as TR quantification by effective regurgitant orifice area and regurgitant volume using the proximal isovelocity surface area method, vena contracta, and hepatic vein reflux¹⁵. According to current literature and recommendations, the leading cause of TR was categorized into primary, CIED-related, atrial or ventricular secondary TR and in case of more than one mechanism as mixed pathology^{8,16–19}. A GE healthcare Vivid E9 or E95 with a M5S(c) 1.5–4.5 MHz or 4Vc-D 3D/4D Phased Array 1.4–5.2 MHz transducer (GE Vingmed, Horton, Norway) was used for echocardiography.

Technical success was defined as successful implantation of the device and retrieval of the delivery system without conversion to surgical or another interventional therapy as well as TR reduction of at least one grade. Outcome parameters comprised TR reduction and all-cause mortality during follow-up.

Computed tomography

CT was performed before intervention during the screening process for TR therapy according to current recommendations^{20,21}. For further analysis of the CTs, we used heart.ai version 1 (Laralab GmbH, Munich, Germany), a cloud-based software platform providing automatic analysis of cardiac CT images for research use (<https://research.heartai-medical.com/>). Heart.ai's computer modeling and simulation methods are based on deep learning techniques. Blood cavities and tissues of the heart were segmented using Convolutional Neural Networks, with different networks focusing on different groups of heart anatomies. The result was a comprehensive segmentation that included the major structures such as the left and right ventricles, as well as finer structures such as tricuspid leaflets. Segmentation was performed for each phase in a cardiac CT series, resulting in a detailed representation of the cardiac anatomy. 3D models of cardiac anatomy were produced from the binary masks of the segmentations using the flying edges algorithm²². Characteristic heart planes for

multiplanar reconstruction views were calculated based on the 3D models, and custom algorithms were used to automatically derive a wide range of measurements, including annulus and right heart dimensions. The 3D models from a given CT series were collated to calculate phase-independent measurements, such as RV stroke volume. Furthermore, this allowed for 4D visualization of the heart's structural dynamics over the cardiac cycle. Automated cardiac CT analysis included the evaluation of right heart morphology and function, as well as TR measurements. Right atrial morphology was measured at the end-systolic phase, right ventricular morphology at end-diastolic phase, tricuspid annulus morphology at both end-systolic and mid-diastolic phases, and tenting parameters at the end-systolic phase. Manual adjustments were made if necessary. Tenting height as well as angles were measured by hand.

Statistical analysis

We used SPSS Statistics version 28 for Windows (IBM Corporation, New York, NY, USA) for statistical analysis. Categorical and ordinal variables were presented in percentages and continuous variables as median with 25th and 75th percentile or mean with standard deviation (depending on their skewness, uniform per variable). Statistical tests for intergroup comparison comprised chi-squared test (categorical parameters), *t*-test (normally distributed, continuous parameters) and Wilcoxon-test or Mann-Whitney-U-test (not normally distributed continuous or ordinal parameters). Outcome predictors were assessed by univariate binary logistic regression analysis with the dependent parameter post-interventional TR grade ≤ 1 . Moreover, receiver operating characteristic (ROC) analysis were conducted to calculate the accuracy of evaluated CT parameters. Correlation of CT and echocardiographic measurements were analysed using Pearson or Spearman's rank correlation, according to the value's distribution. Survival analysis was performed using log-rank test and Kaplan-Meier curves. A *p* value < 0.05 was considered statistically significant.

Ethics approval

The study was approved by the institutional review board of the Charité – Universitätsmedizin Berlin, Berlin, Germany (EA4/218/21 and EA1/043/20).

Results

Between 2019 and 2023, 84 patients with a cardiac CT performed during the screening process were included in our analysis. CTs were conducted 64 (47–91) days prior to interventional therapy. Four patients with CTs not suitable for automated analysis and one patient with a CT performed 7 years before the procedure were excluded. Figure 1 presents the screening and enrolment process of the present study. Baseline characteristics are listed in Table 1. Overall, 32 patients underwent T-TEER and 52 patients PA. Most of the patients were female (63%) and had a median age of 81 (77–83) years. 88% of patients reported a NYHA class III or IV. There were no significant differences regarding baseline characteristics between both groups except for the prevalence of peripheral artery disease and the intake of Sodium-Glucose Transport Protein 2 (SGLT2) inhibitors.

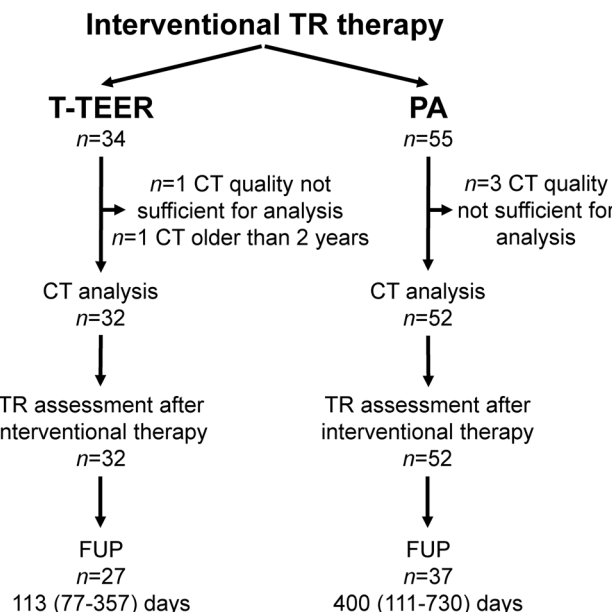


Fig. 1. Flow chart of the study presenting the number of patients with tricuspid regurgitation (TR) who received tricuspid transcatheter edge-to-edge repair (T-TEER) or percutaneous annuloplasty (PA) and follow-up (FUP) examinations.

	T-TEER (n=32)	PA (n=52)	p Value
Female, n (%)	19 (59)	34 (65)	0.579
Age, years (IQR)	82 (78–84)	81 (77–83)	0.287
BMI, kg/m ² (IQR)	24 (22–27)	25 (22–28)	0.235
EUROScore II (IQR)	5.6 (3.5–8.7)	4.5 (3.0–8.4)	0.261
NYHA class			0.112
I, n (%)	0 (0)	0 (0)	
II, n (%)	2 (6)	8 (15)	
III, n (%)	25 (78)	40 (77)	
IV, n (%)	5 (16)	4 (8)	
Leading cause of TR			0.131
Primary TR, n (%)	1 (3)	1 (2)	
Atrial TR, n (%)	24 (75)	28 (54)	
Ventricular TR, n (%)	6 (19)	22 (42)	
CIED-related TR, n (%)	1 (3)	0 (0)	
Mixed pathology, n (%)	0 (0)	1 (2)	
Coronary artery disease, n (%)	12 (38)	30 (58)	0.072
CIED, n (%)	11 (34)	14 (27)	0.468
Atrial fibrillation or flutter, n (%)	28 (88)	50 (96)	0.135
Arterial hypertension, n (%)	26 (81)	45 (87)	0.515
Diabetes mellitus, n (%)	4 (13)	16 (31)	0.082
Stroke, n (%)	8 (25)	9 (17)	0.394
Peripheral artery disease, n (%)	9 (28)	2 (4)	0.001
Chronic obstructive pulmonary disease, n (%)	9 (28)	9 (17)	0.241
History of surgical or percutaneous valve therapy, n (%)	14 (44)	18 (35)	0.402
Serum creatinine, mg/dl (IQR)	1.3 (1.0–1.7)	1.3 (1.0–1.4)	0.652
NT-proBNP, ng/l (IQR)	1919 (1062–3775)	2463 (1711–4206)	0.191
Bilirubin, mg/dl (IQR)	1.0 (0.6–1.6), n=26	0.6 (0.5–1.1), n=33	0.145
Systolic PAP, mmHg \pm SD	38 \pm 14, n=23	41 \pm 13, n=24	0.521
Heart failure therapy			
Diuretics, n (%)	31 (97)	51 (98)	0.726
Beta-blocker, n (%)	29 (91)	43 (83)	0.313
ACE inhibitor or sacubitril/valsartan, n (%)	22 (69)	42 (81)	0.209
Mineralocorticoid receptor antagonist, n (%)	20 (63)	31 (60)	0.793
SGLT2 inhibitor, n (%)	13 (41)	10 (19)	0.033

Table 1. Baseline characteristics. Continuous variables are shown as mean \pm standard deviation (SD, normally distributed) or median with interquartile ranges (IQR, not normally distributed), categorical variables are given as absolute number with percentages. T-TEER, Tricuspid transcatheter edge-to-edge repair; PA, Percutaneous annuloplasty; BMI, Body mass index; EUROScore II; European System for Cardiac Operative Risk Evaluation II; NYHA class, New York Heart Association Class; TR, Tricuspid regurgitation; CIED, Cardiac implantable electronic device; NT-proBNP, N-Terminal pro brain natriuretic peptide; PAP, Pulmonary artery pressure; ACE, Angiotensin-converting enzyme; SGLT2, Sodium-Glucose Transport Protein 2.

CT analysis

CT parameters are presented in Table 2 and shown in Fig. 2. Right ventricular and atrial volumes were increased in the PA compared to the T-TEER group, but these differences did not reach statistical significance. This was consistent with a more pronounced tenting in PA patients, including the tenting angle of the septal leaflet, which was significantly larger in the PA compared to the T-TEER group. The tricuspid valve area and diameters did not differ significantly between the two groups. The distance between the tricuspid annulus and the RCA was larger in patients who underwent PA compared to T-TEER with a significant difference in segment D8 (Fig. 2). 35 patients in the PA (67%) and 23 patients in the T-TEER group (72%) had at least one segment with a distance to the RCA < 6 mm.

Technical success was achieved in 100% of patients. After interventional therapy, PA and T-TEER patients showed a comparable improvement of TR severity (PA: 2.3 ± 0.8 vs. T-TEER: 2.3 ± 0.9 , $p = 0.688$). Detailed TR grades before and after intervention are shown in Fig. 3. For further analysis, we divided both treatment cohorts into patients with a TR grade ≤ 1 and > 1 after intervention. We observed that patients with a post-interventional TR grade ≤ 1 had smaller right ventricular volumes and lower tenting heights, volumes, and angles regardless of PA or T-TEER treatment. This difference reached significance only for tenting height and angles. A comparison of patients with a TR improvement of ≥ 3 grades and < 3 grades showed similar results, except for the right atrial

	T-TEER				PA				<i>p</i> Value for comparison of T-TEER and PA
	Entire cohort (n=32)	Post-interventional TR grade ≤ 1 (n=14)	Post-interventional TR grade > 1 (n=18)	<i>p</i> Value for comparison of TR grade ≤ 1 versus > 1	Entire cohort (n=52)	Post-interventional TR grade ≤ 1 (n=19)	Post-interventional TR grade > 1 (n=33)	<i>p</i> Value for comparison of TR grade ≤ 1 versus > 1	
LVEF, % ± SD	58 ± 11	56 ± 10	59 ± 11	0.382	59 ± 11	57 ± 13	60 ± 10	0.350	0.673
RA volume, ml ± SD	291 ± 96	296 ± 77	287 ± 111	0.807	307 ± 98	287 ± 69	320 ± 111	0.197	0.448
RA diameter (four-chamber view), mm ± SD	70 ± 10	71 ± 8	70 ± 11	0.743	70 ± 9	68 ± 9	71 ± 10	0.223	0.896
RA height, mm ± SD	75 ± 11	76 ± 11	74 ± 11	0.607	77 ± 11	76 ± 9	77 ± 12	0.606	0.388
RVEF, % ± SD	55 ± 8	56 ± 10	55 ± 7	0.912	55 ± 8	54 ± 9	55 ± 8	0.714	0.755
RVSV, ml (IQR)	125 (100–150)	113 (104–149)	136 (97–154)	0.411	134 (112–162)	131 (97–149)	147 (117–169)	0.078	0.246
RV EDV, ml (IQR)	224 (183–293)	209 (169–294)	236 (185–315)	0.428	248 (199–297)	208 (172–263)	272 (229–310)	0.079	0.570
RV ESV, ml (IQR)	97 (66–140)	95 (63–144)	98 (72–149)	0.511	110 (77–139)	99 (75–112)	114 (87–146)	0.108	0.470
RV height, mm ± SD	61 ± 13	61 ± 13	61 ± 13	0.950	64 ± 10	65 ± 7	64 ± 11	0.812	0.164
RV length, mm (IQR)	87 (76–97)	84 (73–94)	87 (79–101)	0.254	85 (80–91)	84 (78–91)	86 (80–91)	0.436	0.941
TV area mid-diastolic, mm ² (IQR)	1798 (1550–2049)	1720 (1594–2151)	1832 (1492–2005)	0.732	1701 (1556–2013), n=50	1589 (1394–1921), n=18	1720 (1657–2037), n=32	0.150	0.683
TV perimeter mid-diastolic, mm ± SD	151 ± 18	151 ± 16	151 ± 21	0.946	149 ± 15, n=50	147 ± 16, n=18	151 ± 15, n=32	0.391	0.613
SL TV diameter mid-diastolic, mm ± SD	48 ± 7	49 ± 6	48 ± 7	0.668	49 ± 5, n=50	48 ± 6, n=18	49 ± 5, n=32	0.503	0.861
AP TV diameter mid-diastolic, mm (IQR)	47 (43–52)	48 (43–51)	47 (41–53)	0.933	45 (43–51), n=50	45 (41–48), n=18	45 (43–51), n=32	0.337	0.353
Tenting height, mm (IQR)	8 (5–11)	6 (4–8)	9 (8–12)	0.004	10 (7–12)	9 (6–11)	11 (8–13)	0.131	0.098
Tenting volume, ml (IQR)	3 (1–5), n=28	2 (1–3), n=10	4 (1–9)	0.150	3 (1–6), n=50	2 (1–4)	4 (2–7), n=31	0.099	0.715
Tenting angle septal leaflet, ° (IQR)	17 (10–26)	16 (8–20)	24 (15–27)	0.033	27 (16–38), n=51	22 (14–34)	29 (19–41), n=32	0.070	0.010
Tenting angle anterior leaflet, ° (IQR)	23 (16–34)	18 (9–30)	26 (22–35)	0.023	26 (19–33), n=51	25 (18–32)	27 (19–36), n=32	0.370	0.304
Tenting angle posterior leaflet, (IQR)	23 (14–31)	19 (8–28)	26 (19–38)	0.071	26 (17–36), n=51	22 (17–32)	27 (16–40), n=32	0.320	0.362
Mean distance TA to RCA (D1–8), mm ± SD	8.4 ± 2.6	8.5 ± 2.5	8.4 ± 2.7	0.884	9.1 ± 2.2	8.9 ± 2.1	9.1 ± 2.2	0.754	0.231
Mean number of segments with proximity to the RCA* per patient, n (IQR)	3 (0–4)	3 (0–4)	3 (0–4)	0.969	2 (0–3)	2 (0–3)	1 (0–3)	0.751	0.148

Table 2. Automated computed tomography analysis. *Proximity to the RCA was defined as a distance < 6 mm. Continuous variables are shown as mean ± standard deviation (SD, normally distributed) or median with interquartile ranges (IQR, not normally distributed). T-TEER, Tricuspid transcatheter edge-to-edge repair; PA, Percutaneous annuloplasty; LVEF, Left ventricular ejection fraction; RA, Right atrial; RVEF, Right ventricular ejection fraction; RVSV, Right ventricular stroke volume; RV EDV, Right ventricular end-diastolic volume; RV ESV, Right ventricular end-systolic volume; RV height, Right ventricular height (corresponds to the length of the RV measured perpendicular to the tricuspid valve plane); RV length, Right ventricular length (corresponds to the length of the RV from apex to base); TV, Tricuspid valve; SL, Septolateral; AP, Anteroposterior; TA, Tricuspid annulus; RCA, Right coronary artery.

diameter in the two-chamber view in the PA group (TR improvement of ≥ 3 grades: 102 (95–109) mm vs. TR improvement < 3 grades: 92 (83–100) mm, *p* = 0.019).

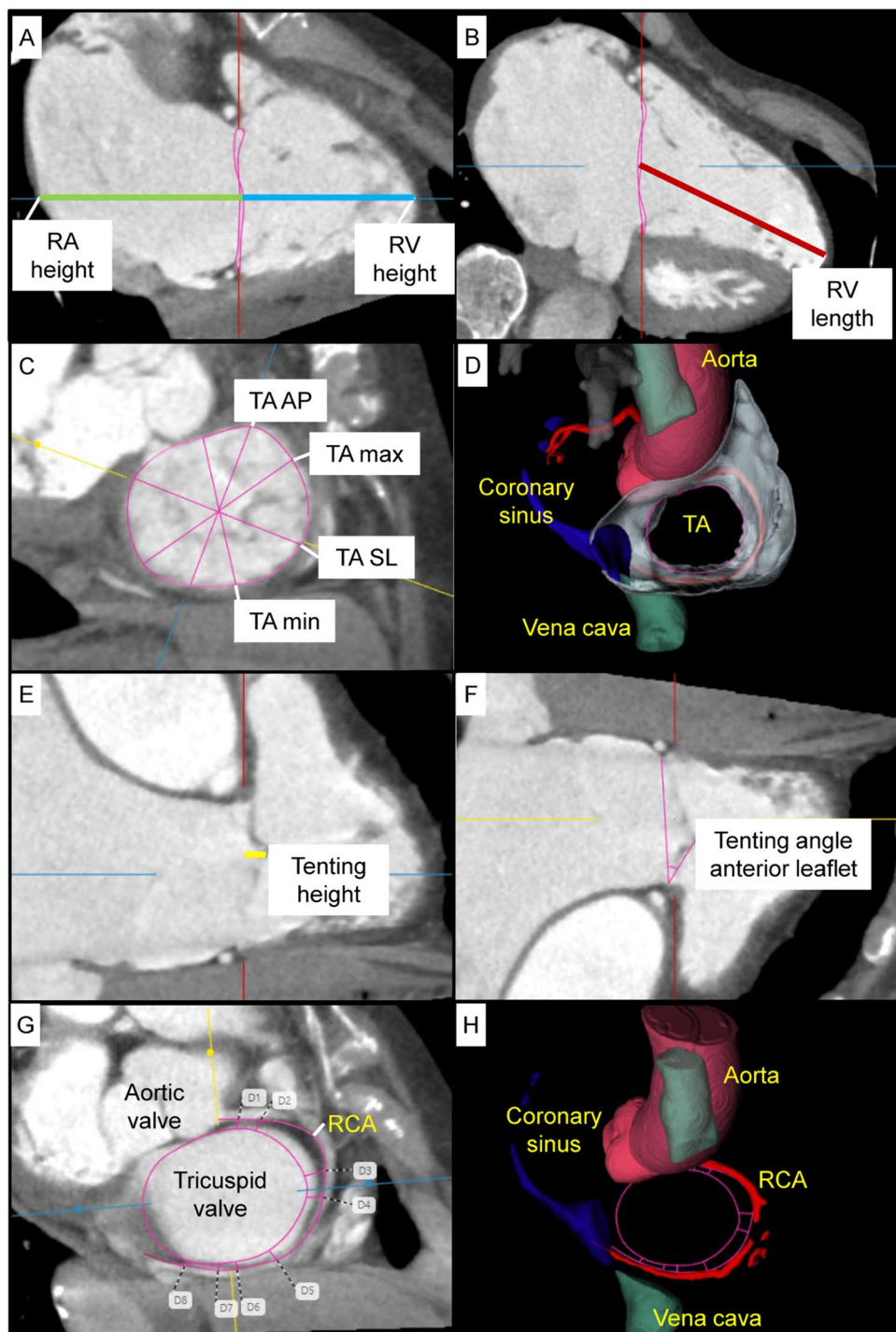


Fig. 2. Computed tomography (CT) analysis of right atrial (RA) and right ventricular (RV) height (A), RV length (B), tricuspid annulus (TA) with antero-posterior (AP), septo-lateral (SL), minimal (min) and maximal (max) diameter (C, D), tenting height (E), tenting angle of the anterior leaflet (F), and distance between tricuspid annulus and right coronary artery (RCA, G, H).

Predictors of post-interventional TR reduction

In the T-TEER group, the tenting height and the tenting angle of the anterior leaflet predicted a post-interventional TR grade ≤ 1 (tenting height: odds ratio [OR] 0.707 [95% confidence interval [CI] 0.537–0.931]; tenting angle: OR 0.919 [95% CI 0.850–0.993]). Neither right atrial volume, right ventricular end-systolic and end-diastolic volume, RVEF, tenting angle of the septal and posterior leaflet, tenting volume nor end-systolic and mid-diastolic tricuspid valve area as well as a more circular shape of the tricuspid annulus or the sphericity

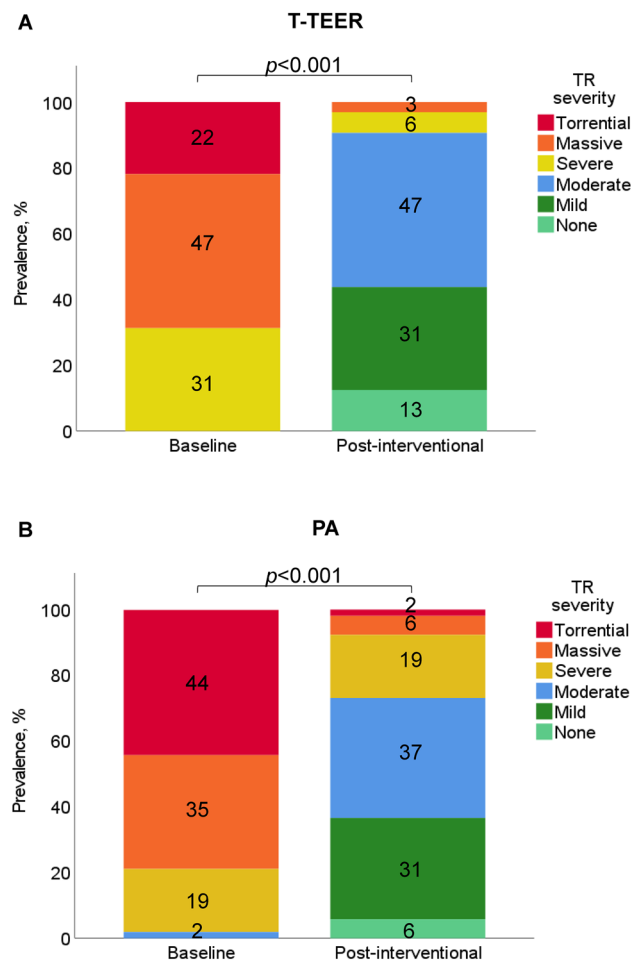


Fig. 3. Severity of tricuspid regurgitation (TR) before and immediately after (A) tricuspid transcatheter edge-to-edge repair (T-TEER) or (B) percutaneous annuloplasty (PA).

index predicted a TR grade ≤ 1 after T-TEER. Similarly, none of the mentioned parameters predicted a TR grade ≤ 1 after PA.

Furthermore, we conducted a ROC analysis with tenting height, volume, and angles to predict the outcome TR grade > 1 after intervention (Fig. 4). The tenting height showed the best diagnostic accuracy among evaluated parameters with an AUC of 0.756 (95% CI 0.560–0.951) in the T-TEER and 0.658 (95% CI 0.501–0.815) in the PA group. To determine post-interventional TR grade > 1 , the threshold of 6.8 mm tenting height corresponded to a sensitivity of 83% and specificity of 70% in the T-TEER group, while the cut-off value of 9.2 mm was associated with a sensitivity and specificity of 68% in the PA group (Fig. 5).

Correlation of CT and echocardiographic measurements

CT and echocardiographic measurements showed a significant correlation regarding left ventricular ejection fraction (LVEF, Pearson 0.574, $p < 0.001$, $n = 84$), right atrial diameter in the four-chamber view (Pearson 0.619, $p < 0.001$, $n = 84$), right ventricular length (Spearman-Rho 0.648, $p < 0.001$, $n = 83$) and tenting height (Pearson 0.603, $p < 0.001$, $n = 84$). Echocardiographic parameters are listed in Table 3.

Long-term follow-up

The mean follow-up duration of 41 patients with a post-interventional TR grade > 1 was 370 ± 265 days, and that of 23 patients with a post-interventional TR grade ≤ 1 was 331 ± 300 days. Among the first group, five patients (12%) died during the follow-up, including two due to cardiovascular reasons. One patient (4%) with a post-interventional TR grade ≤ 1 died due to non-cardiovascular reasons 1046 days after intervention ($p = 0.124$ for intergroup comparison, Fig. 6).

Discussion

The present study compared right heart morphology and function assessed by cardiac CT of patients who underwent T-TEER or PA and evaluated predictors of TR reduction after interventional therapy using automated deep learning CT algorithms. The principal findings include:

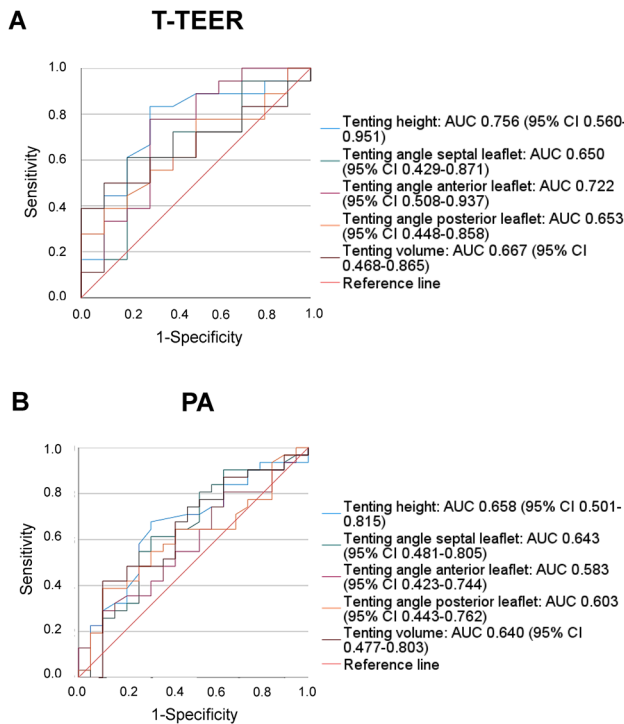


Fig. 4. Receiver operating characteristic (ROC) analysis with area under the curve (AUC) and confidence interval (CI) of tenting height, tenting angle of the septal, anterior, and posterior leaflet and tenting volume. Patients after tricuspid transcatheter edge-to-edge repair (T-TEER) are presented in (A), patients after percutaneous annuloplasty (PA) in (B).

- (i) PA patients presented larger right heart volumes and greater tenting. Nevertheless, PA and T-TEER resulted in a comparable TR improvement of, on average, 2–3 grades.
- (ii) Expectedly (since safe distance to the RCA is a prerequisite for PA), the distance between the tricuspid annulus and the RCA was larger in the PA compared to the T-TEER group. However, 67% of patients who underwent PA had at least one segment which showed proximity to the RCA (defined as a distance < 6 mm).
- (iii) Patients with a post-interventional TR grade ≤ 1 had lower tenting heights and angles. In the T-TEER group, the tenting height and angle of the anterior leaflet were associated with a post-interventional TR grade ≤ 1 . We identified a tenting height threshold of 6.8 mm for T-TEER and 9.2 mm for PA to determine a post-interventional TR grade > 1 .
- (iv) Patients with a post-interventional TR grade > 1 showed a numerically higher mortality (12%) compared to patients with a TR grade ≤ 1 (4%).

Right heart anatomy and function

In the present study, automated deep learning CT assessment was used to analyze right heart morphology and function. Measured median tricuspid valve area was slightly smaller compared to previous studies. Ingraham et al. reported an area of $19.5 \pm 4.6 \text{ cm}^2$ in patients who underwent surgical or interventional TR therapy and an area of $21.2 \pm 2.25 \text{ cm}^2$ in TR patients with medical treatment²³. In the current study, patients with a residual TR grade > 1 exhibited slightly more enlarged right heart chambers compared to those with a TR grade ≤ 1 . This is in line with results from mitral edge-to-edge repair (M-TEER). After the results of the COAPT and the MITRA-FR study, M-TEER is recommended for patients with left ventricular end-systolic diameter ≤ 70 mm according to the European Society of Cardiology (ESC) guideline on valvular heart disease (class IIa)^{24,25}. Another relevant anatomical aspect for device selection is the distance between RCA and tricuspid annulus⁸. In clinical practice, a distance of at least 6 mm is recommended for PA treatment. However, 67% of patients in the PA and 72% of patients in the T-TEER group had at least one segment with a distance < 6 mm to the RCA. In the PA group, two patients required coronary intervention due to RCA perforation (3.8%), which was slightly higher than the reported prevalence by Nickening et al.²⁶. Nevertheless, none of the segments for the two patients were at a distance < 6 mm. Therefore, further studies should investigate the minimum distance required and whether other risk factors contribute to perforation.

In addition to morphology, right ventricular function is an important outcome predictor in patients who underwent T-TEER or PA¹¹. Patients referred for surgical or interventional TR therapy exhibited better right ventricular function in comparison to those undergoing medical treatment²³. In the present study, mean RVEF assessed by CT and mean tricuspid annular plane systolic excursion (TAPSE) as well as right ventricular

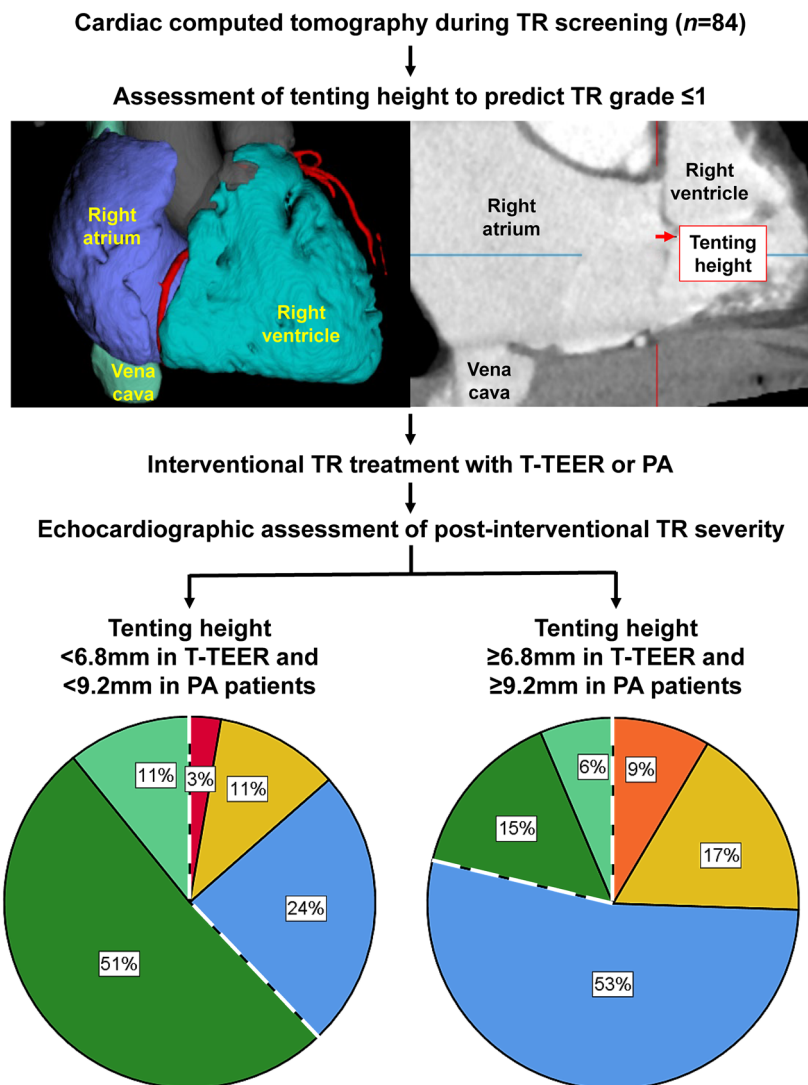


Fig. 5. Tenting height assessed by computed tomography (CT) was associated with a higher risk of residual TR after tricuspid transcatheter edge-to-edge repair (T-TEER) and percutaneous annuloplasty (PA). In ROC analysis, the threshold of 6.8 mm tenting height corresponded to a sensitivity of 83% and specificity of 70% in the T-TEER group and the threshold of 9.2 mm to a sensitivity and specificity of 68% in the PA group to determine TR grade > 1 post-interventional.

fractional area change (RV FAC) measured by echocardiography were in a normal range in T-TEER and PA patients at baseline.

Tenting in TR

A significant tenting predominantly occurs in advanced and ventricular TR, but not in atrial TR as described by Schlotter et al.¹⁷. Consistent with this, patients with more pronounced tenting showed larger right ventricular end-diastolic volumes in the present study. Ingraham et al. observed an increased tenting height among patients undergoing medical management in contrast to those referred for surgical or interventional TR therapy²³. CT measurements of mean tenting height were comparable to our values²³. However, patients with a post-interventional TR > 1 exhibited similar (T-TEER) and slightly larger (PA) tenting heights compared to medically managed patients²³. Nevertheless, a successful interventional treatment was reached despite elevated tenting heights in the current study. A TR reduction of at least one grade was achieved in all patients. In the T-TEER group, up to three devices were implanted in patients with a post-interventional TR grade ≤ 1 (one device: 7%, two devices: 71%, three devices: 21%) and up to two devices in patients with a post-interventional TR grade > 1 (one device: 22%, two devices: 78%, $p = 0.080$). In M-TEER, tenting is a known risk factor for single leaflet device attachments (SLDA)²⁷. Two patients of our cohort (6%) presented with SLDA between the posterior and septal leaflet a few days after T-TEER. In both cases, the tenting heights formed by the posterior and septal leaflets were 0 and 6 mm, respectively. Thus, a causal relationship with detachment a few days after T-TEER remains unclear.

	T-TEER (n=32)	PA (n=52)	p Value
LVEF, % \pm SD	51 \pm 8	53 \pm 11	0.339
RVD basal, mm \pm SD	50 \pm 10	49 \pm 8	0.642
RVD length, mm \pm SD	68 \pm 13, n=31	69 \pm 10	0.694
RAD, mm \pm SD	55 \pm 10	55 \pm 12	0.970
TAPSE, mm \pm SD	18 \pm 4, n=30	18 \pm 6, n=51	0.608
RV FAC, % \pm SD	45 \pm 11, n=28	41 \pm 9, n=51	0.175
Tenting height, mm \pm SD	3 \pm 3	6 \pm 4	<0.001
Gap ATL STL, mm (IQR)	4 (2–6), n=28	5 (3–6), n=37	0.288
Gap PTL STL, mm \pm SD	5 \pm 2, n=29	5 \pm 3, n=37	0.695

Table 3. Echocardiographic measurements. Continuous variables are shown as mean \pm standard deviation (SD, normally distributed) or median with interquartile ranges (IQR, not normally distributed). T-TEER, Tricuspid transcatheter edge-to-edge repair; PA, Percutaneous annuloplasty; LVEF, Left ventricular ejection fraction; RVD, Right ventricular diameter; RAD, Right atrial diameter in the four-chamber view; TAPSE, Tricuspid annular plane systolic excursion; RV FAC, Right ventricular fractional area change; ATL, Anterior tricuspid leaflet; STL, Septal tricuspid leaflet; PTL, Posterior tricuspid leaflet.

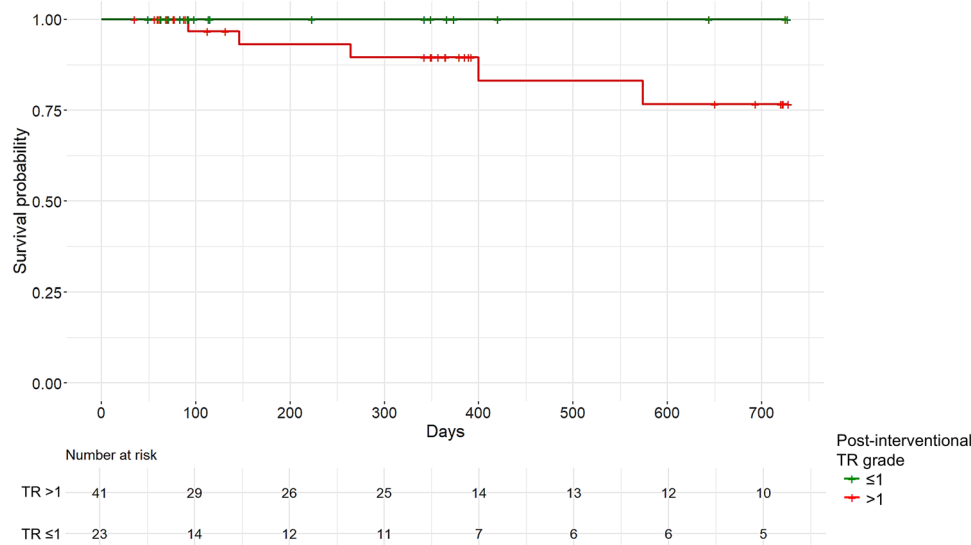


Fig. 6. Kaplan–Meier curves of survival probability of patients with a post-interventional TR grade > 1 and ≤ 1 during a follow-up of 24 months. TR Tricuspid regurgitation.

Moreover, more pronounced tenting was associated with TR grade > 1 after intervention in our study. This result is in line with findings from surgical annuloplasty in TR²⁸. Tenting volume measured by 3D echocardiography was a predictor of residual TR after surgery²⁸. In contrast, in the present study, tenting volume measured by CT had a lower AUC compared to tenting height in ROC analysis.

An alternative approach for patients with a significant tenting is orthotopic valve implantation²³. The maximal mid-diastolic annulus diameter in T-TEER patients with a postinterventional TR grade > 1 was 52 (48–56) mm and in PA patients 51 (49–55) mm. As an example, the EVOQUE® valve (Edwards Lifesciences, Irvine, CA, USA) is available up to a diameter of 52 mm which reflects the unmet need for larger devices²³. Nevertheless, besides technical advancements, TR patients should potentially be treated at earlier stages of the disease to prevent significant right ventricular enlargement and progression of tenting²³. Further relevant predictors of residual TR comprised the leaflet-to-annulus index and the positioning of leads from CIEDs after T-TEER^{29,30}.

In comparison to echocardiography, we observed larger values of tenting height measured by CT, although both measurements showed a correlation. One possible explanation might be the varying visibility of the leaflets in both modalities and the use of different phases as well as imaging perspectives with visualization of different leaflets. CT measurements were conducted at end-systolic phase using a two-chamber view, while echocardiographic parameters were evaluated in a late systolic phase in a four-chamber view. Tenting height measured by echocardiography also predicted a post-interventional TR grade ≤ 1 after T-TEER (OR 0.736 [95% CI 0.546–0.993]) but not after PA (OR 0.972 [95% CI 0.854–1.108]). The calculated AUC of echocardiographic

tenting height was lower compared to CT analysis in both groups (T-TEER AUC 0.720 [95% CI 0.538–0.902] and PA AUC 0.510 [95% CI 0.352–0.669]).

Limitations

Our study is limited by its single-center observational design. Results should be interpreted as hypothesis-generating due to limited case numbers. In a few patients, the measurement of tenting height using CT was challenging due to inadequate visualization of the leaflets. Furthermore, diameters of the right heart and tricuspid annulus are volume load dependent, which may lead to different measurements at screening (echocardiography and CT) and intervention. In addition to methodological limitations, both PA and T-TEER address different mechanism and were therefore used in patients with different anatomical characteristics such as atrial and ventricular TR. This must be taken into account when interpreting the results.

Conclusion

Automated CT assessment of the right heart morphology and function as well as the tricuspid valve has the potential to guide decision making before interventional therapy of TR but needs confirmation in prospective studies. Significant tenting may identify patients with a high risk for residual TR after T-TEER and PA.

Data availability

The data that support the findings of this study are available from the corresponding author upon reasonable request.

Received: 7 December 2023; Accepted: 21 August 2024

Published online: 27 August 2024

References

- Offen, S., Playford, D., Strange, G., Stewart, S. & Celermajer, D. S. Adverse prognostic impact of even mild or moderate tricuspid regurgitation: Insights from the National Echocardiography Database of Australia. *J. Am. Soc. Echocardiogr.* **35**(8), 810–817 (2022).
- Topilsky, Y. *et al.* Burden of tricuspid regurgitation in patients diagnosed in the community setting. *JACC Cardiovasc. Imaging.* **12**(3), 433–442 (2019).
- Kilic, A., Saha-Chaudhuri, P., Rankin, J. S. & Conte, J. V. Trends and outcomes of tricuspid valve surgery in North America: An analysis of more than 50,000 patients from the Society of Thoracic Surgeons database. *Ann. Thorac. Surg.* **96**(5), 1546–1552 (2013).
- Taramasso, M. *et al.* The International Multicenter TriValve Registry: Which patients are undergoing transcatheter tricuspid repair?. *JACC Cardiovasc. Interv.* **10**(19), 1982–1990 (2017).
- Nickenig, G. *et al.* 6-Month outcomes of tricuspid valve reconstruction for patients with severe tricuspid regurgitation. *J. Am. Coll. Cardiol.* **73**(15), 1905–1915 (2019).
- Lurz, P. *et al.* Transcatheter edge-to-edge repair for treatment of tricuspid regurgitation. *J. Am. Coll. Cardiol.* **77**(3), 229–239 (2021).
- Kodali, S. *et al.* Feasibility study of the transcatheter valve repair system for severe tricuspid regurgitation. *J. Am. Coll. Cardiol.* **77**(4), 345–356 (2021).
- Praz, F. *et al.* Transcatheter treatment for tricuspid valve disease. *EuroIntervention.* **17**(10), 791–808 (2021).
- Russo, G. *et al.* Challenges and future perspectives of transcatheter tricuspid valve interventions: Adopt old strategies or adapt to new opportunities?. *Eur. J. Heart Fail.* **24**(3), 442–454 (2022).
- Hahn, R. T. *et al.* Multimodality imaging of right heart function: JACC scientific statement. *J. Am. Coll. Cardiol.* **81**(19), 1954–1973 (2023).
- Tanaka, T. *et al.* Right ventricular ejection fraction assessed by computed tomography in patients undergoing transcatheter tricuspid valve repair. *Eur. Heart J. Cardiovasc. Imaging.* **24**, 1501–1508 (2023).
- Mattig, I. B. F. *et al.* Comparison of procedural characteristics of percutaneous annuloplasty and edge-to-edge repair for the treatment of severe tricuspid regurgitation. *Front. Cardiovasc. Med.* **10**, 123237 (2023).
- Lang, R. M. *et al.* Recommendations for cardiac chamber quantification by echocardiography in adults: An update from the American Society of Echocardiography and the European Association of Cardiovascular Imaging. *Eur. Heart J. Cardiovasc. Imaging.* **16**(3), 233–270 (2015).
- Lancellotti, P. *et al.* Multi-modality imaging assessment of native valvular regurgitation: An EACVI and ESC council of valvular heart disease position paper. *Eur. Heart J. Cardiovasc. Imaging.* **23**(5), e171–e232 (2022).
- Hahn, R. T. & Zamorano, J. L. The need for a new tricuspid regurgitation grading scheme. *Eur. Heart J. Cardiovasc. Imaging.* **18**(12), 1342–1343 (2017).
- Sade, L. E. *et al.* How to assess severe tricuspid regurgitation by echocardiography?. *Eur. Heart J. Cardiovasc. Imaging.* **23**(10), 1273–1276 (2022).
- Schlotter, F. *et al.* Atrial functional tricuspid regurgitation: Novel definition and impact on prognosis. *Circ. Cardiovasc. Interv.* **15**(9), e011958 (2022).
- Florescu, D. R. *et al.* Right heart chambers geometry and function in patients with the atrial and the ventricular phenotypes of functional tricuspid regurgitation. *Eur. Heart J. Cardiovasc. Imaging.* **23**(7), 930–940 (2022).
- Russo, G. *et al.* Characteristics and outcomes of patients with atrial versus ventricular secondary tricuspid regurgitation undergoing tricuspid transcatheter edge-to-edge repair—Results from the TriValve registry. *Eur. J. Heart Fail.* **25**(12), 2243–2251 (2023).
- Hell, M. M. *et al.* Computed tomography imaging needs for novel transcatheter tricuspid valve repair and replacement therapies. *Eur. Heart J. Cardiovasc. Imaging.* **22**(6), 601–610 (2021).
- Pulerwitz, T. C. *et al.* Optimizing cardiac CT protocols for comprehensive acquisition prior to percutaneous MV and TV repair/replacement. *JACC Cardiovasc. Imaging.* **13**(3), 836–850 (2020).
- Schroeder, W., Maynard, R. & Geveci, B. Flying edges: A high-performance scalable isocontouring algorithm. In *2015 IEEE 5th Symposium on Large Data Analysis and Visualization (LDAV)*; 25–26 October 2015 (IEEE, 2015).
- Ingraham, B. S. *et al.* Analysis of cardiac computed tomography anatomy in patients with severe tricuspid regurgitation considered for transcatheter intervention. *Struct. Heart.* **7**(1), 100100 (2023).
- McDonagh, T. A. *et al.* 2021 ESC Guidelines for the diagnosis and treatment of acute and chronic heart failure. *Eur. Heart J.* **42**(36), 3599–3726 (2021).
- Zalawadiya, S. K., Gonzales, H. M., Goel, K. & Lindenfeld, J. MitraClip for secondary mitral regurgitation: Patient selection. *Prog. Cardiovasc. Dis.* **73**, 67–75 (2022).

26. Nickenig, G. *et al.* Thirty-day outcomes of the Cardioband tricuspid system for patients with symptomatic functional tricuspid regurgitation: The TriBAND study. *EuroIntervention* **17**(10), 809–817 (2021).
27. Kitamura, M., Besler, C., Lurz, P. & Noack, T. Bail-out edge-to-edge mitral repair for an acute single leaflet device attachment: A case report. *Eur. Heart J. Case Rep.* **5**(4), ytab147 (2021).
28. Min, S. Y. *et al.* Geometric changes after tricuspid annuloplasty and predictors of residual tricuspid regurgitation: A real-time three-dimensional echocardiography study. *Eur. Heart J.* **31**(23), 2871–2880 (2010).
29. Tanaka, T. *et al.* Leaflet-to-anulus index and residual tricuspid regurgitation following tricuspid transcatheter edge-to-edge repair. *EuroIntervention* **18**(2), e169–e178 (2022).
30. Lurz, J. *et al.* Safety and efficacy of transcatheter edge-to-edge repair of the tricuspid valve in patients with cardiac implantable electronic device leads. *JACC Cardiovasc. Interv.* **12**(20), 2114–2116 (2019).

Acknowledgements

Isabel Mattig is participant in the BIH Charité Clinician Scientist Program funded by the Charité – Universitätsmedizin Berlin and the Berlin Institute of Health at Charité (BIH).

Author contributions

I.M.: Conceptualization, data curation, investigation, methodology, project administration, visualization, writing—original draft and revision. E.R.D.: Data curation, writing—original draft. K.F.: Data curation, methodology, writing—original draft. A.L.: Supervision, writing—original draft. M.D.: Supervision, writing—original draft. K.S.: Supervision, writing—original draft. H.D.: Conceptualization, data curation, investigation, methodology, project administration, supervision, writing—original draft, writing—review and editing.

Funding

Open Access funding enabled and organized by Projekt DEAL.

Competing interests

The authors declare no competing interests.

Additional information

Correspondence and requests for materials should be addressed to H.D.

Reprints and permissions information is available at www.nature.com/reprints.

Publisher's note Springer Nature remains neutral with regard to jurisdictional claims in published maps and institutional affiliations.

Open Access This article is licensed under a Creative Commons Attribution 4.0 International License, which permits use, sharing, adaptation, distribution and reproduction in any medium or format, as long as you give appropriate credit to the original author(s) and the source, provide a link to the Creative Commons licence, and indicate if changes were made. The images or other third party material in this article are included in the article's Creative Commons licence, unless indicated otherwise in a credit line to the material. If material is not included in the article's Creative Commons licence and your intended use is not permitted by statutory regulation or exceeds the permitted use, you will need to obtain permission directly from the copyright holder. To view a copy of this licence, visit <http://creativecommons.org/licenses/by/4.0/>.

© The Author(s) 2024